The International Journal of Advanced Manufacturing Technology (2018) 98:2429–2438
https://doi.org/10.1007/s00170-018-2390-2

ORIGINAL ARTICLE

Electromechanical impedance (EMI) technique as alternative to monitor workpiece surface damages after the grinding operation

Rosemar Batista da Silva[1] · Fabio Isaac Ferreira[2] · Fabrício Guimares Baptista[2] · Paulo Roberto de Aguiar[2] · Rodrigo de Souza Ruzzi[1] · Henrique Butzlaff Hubner[1] · Maria da Penha Cindra Fonseca[3] · Eduardo Carlos Bianchi[4]

Received: 23 February 2018 / Accepted: 28 June 2018 / Published online: 9 July 2018

Abstract

Electromechanical impedance (EMI) technique has been employed in detection of structural failure in civil and mechanical structures because of its non-destructive property and easy implementation of small and inexpensive piezoelectric transducers that are attached to the structures, which lead to cost reduction as well as lesser dependence of manual inspection methods. In this technique, the capsule is excited by applying a sinusoidal voltage to generate waves to propagate throughout the structure. From the impedance signature of the structure without any damage, any structural change can be detected by measuring the electrical impedance of the piezoelectric (PZT) patch. Based on its real potentiality and because of its non-destructive characteristics, this work aimed to employ the EMI technique as the first alternative to monitor workpiece surface damages after grinding operation with a conventional abrasive grinding wheel. EMI measurements were performed by using a low-cost PZT transducer and under controlled environmental conditions. Microhardness and surface roughness of the machined surfaces, as well as grinding power, were also measured to detect any damage in the machined surface and to stablish relationship with the EMI technique. From the damage indices root mean square deviation (RMSD) and correlation coefficient deviation metric (CCDM), surface alterations on the ground surfaces were inferred by the EMI method. Also, it was observed a good correlation between the EMI technique and the other output parameters that were investigated in this work, such as surface roughness and power grinding, thereby posing as a non-destructive, low-cost, and viable technique to monitor workpiece surface damages in the grinding operation.

Keywords Grinding · Surface integrity · Non-destructive technique · Electromechanical impedance · Microhardness · Surface roughness · Grinding power · Piezoelectric transducers

✉ Rosemar Batista da Silva
rosemar.silva@ufu.br

Fabio Isaac Ferreira
fab.kf@hotmail.com

Fabrício Guimares Baptista
fabriciogb@feb.unesp.br

Paulo Roberto de Aguiar
aguiarpr@feb.unesp.br

Rodrigo de Souza Ruzzi
rodrigo.ruzzi@ufu.br

Henrique Butzlaff Hubner
henrique.hubner@ufu.br

Maria da Penha Cindra Fonseca
mcindra@vm.uff.br

Eduardo Carlos Bianchi
bianchi@feb.unesp.br

[1] School of Mechanical Engineering, Federal University of Uberlandia (UFU), Av. João Naves de Ávila, 2121 – Campus Santa Mônica, Uberlândia, MG CEP: 38408-100, Brazil

[2] Department of Electrical Engineering, Faculty of Engineering Bauru (FEB), São Paulo State University (UNESP), São Paulo, Brazil

[3] School of Mechanical, Federal University Fluminense (UFF), Niterói, Brazil

[4] Department of Mechanical Engineering, Faculty of Engineering Bauru (FEB), São Paulo State University (UNESP), São Paulo, Brazil

1 Introduction

The grinding operation is generally the first choice when combination of low surface roughness and high accuracy of components is required. However, this process presents some peculiarities that demand special attention when compared to other machining processes like milling and turning, for instance. One peculiarity is related to the workpiece material that is more susceptible to occurrence of thermal damages. Because of low values of depth of cut, chips are generated with small sessions and refractory properties of the typically used conventional abrasive materials used in grinding wheels. For instance, the thermal conductivity of the aluminum oxide is a half of that for AISI 1020 steel [1]; most of the heat that is generated during grinding flows to the workpiece material. Such phenomenon leads to use of cutting fluids that is practically indispensable in this process to cool the workpiece material surface and avoid thermal damages such as burning, cracks, metallurgical alterations, and tensile residual stress [2]. According to Malkin and Guo [3], surface roughness, thermal damage, and residual stresses are the primary factors to ensure surface integrity, with exception of workpiece burn that, in steels, is characterized by bluish temper colors and is visible on the workpiece surface. Thermal damages usually can be detected by destructive techniques, especially through metallurgical examination of ground surfaces. In-process monitoring of the grinding power, a non-destructive technique, can be also a good technique for estimating temperatures in grinding zone as well as to control thermal damages, but it needs some support from temperature measuring techniques which in general are restricted to the laboratory and cannot be applied in a production environment. Because of the short contact time between the abrasive wheel and the workpiece surface, dynamic response of the thermocouple in determination of grinding temperatures is still a limiting factor. A summary of standard techniques to assess surface integrity of machined surfaces can be found elsewhere [4]. Ullah et al. [5] described a theoretical model to predict the workpiece surface topography after multi-pass grinding and affirmed that there is still a gap between analytical and experimental results that can be used to develop a more comprehensive grinding mechanism model. In other research, Caggiano and Teti [6] evaluated the surface integrity of Rene 80, nickel-based, alloy after grinding with three different CBN grinding wheels in different cutting conditions. In addition to the measurements of surface roughness and grinding power, these authors used the fluorescent penetrant inspection (FPI) technique to detect presence of cracks on the machined surface and visual inspections to guarantee production of aircraft components in compliance to stipulated requirements. Tensile testing and X-ray diffraction are also options to measure tensile strength and ductility and residual stresses of machined components as well. The first technique is a destructive method while the second one is generally limited to a spatial resolution of about 1 μm and by high cost of the instrumentation equipment [7]. So, techniques that combine non-destructive characteristics, rapidness, and low cost to monitor and to prevent thermal damages in engineered parts are always pursued. In this sense, electromechanical impedance (EMI) emerges as a promising non-destructive method to help in evaluation of detection of thermal damages in machined parts. EMI technique consists of easy implementation of small and inexpensive piezoelectric (PZT) sensors that are attached on the structures, which lead to cost reduction as well as lesser dependence of manual and destructive inspection methods [8, 9]. Operation and instrumentation details of the EMI technique are described elsewhere by Baptista et al. [9] and Bhalla and Soh [10]. After the bonding of the PZT sensor, it is electrically excited by means of a meter of the parameters inductance (L), capacitance (C), and resistance (R), that is abbreviated by LCR, or also by an impedance analyzer. A harmonic voltage signal is applied by the LCR across the PZT patch at an appropriate frequency range, at specified intervals, in sweep mode that results in deformations in the PZT patch as well as in the local area of the host structure around it [10]. The PZT exciting produces an interaction between the mechanical impedance of the host structure and the electrical impedance of the sensor [9]. According to these authors, in the EMI method, the PZT sensor operates simultaneously as an actuator and as a sensor, and the electrical impedance signature (in function of the frequency response) is obtained in the same frequency range within which the excitation signal is generated. Thus, from the impedance signature of the structure (corresponding to the workpiece material in machining) without any damage, any structural change can be detected by measuring the electrical impedance of the PZT patch, i.e., the signatures are collected and compared with the baseline signature.

The comparison between signals of a structure without any damage and one other with damage is performed by means of the damage indices. In the research work carried out by Marchi et al. [11] about monitoring the surface integrity of a low carbon steel via EMI technique during grinding, the authors employed the most commonly damage indices reported in the specific literature: the root mean square deviation (RMSD) and correlation coefficient deviation metric (CCDM), which are calculated by Eqs. 1 and 2, respectively.

$$\mathrm{RMSD} = \sum_{k=\omega_\mathrm{I}}^{\omega_\mathrm{F}} \sqrt{\frac{\left[Z_{\mathrm{E,D}}(k) - Z_{\mathrm{E,H}}(k)\right]^2}{Z_{\mathrm{E,H}}^2(k)}} \tag{1}$$

$$\mathrm{CCDM} = 1 - \frac{\sum_{k=\omega_\mathrm{I}}^{\omega_\mathrm{F}} \left[Z_{\mathrm{E,H}}(k) - \overline{Z}_{\mathrm{E,H}}\right]\left[Z_{\mathrm{E,D}}(k) - \overline{Z}_{\mathrm{E,D}}\right]}{\sqrt{\sum_{k=\omega_\mathrm{I}}^{\omega_\mathrm{F}} \left[Z_{\mathrm{E,H}}(k) - \overline{Z}_{\mathrm{E,H}}\right]^2} \sqrt{\sum_{k=\omega_\mathrm{I}}^{\omega_\mathrm{F}} \left[Z_{\mathrm{E,D}}(k) - \overline{Z}_{\mathrm{E,D}}\right]^2}} \tag{2}$$

where $Z_{\mathrm{E,H}}(k)$ and $Z_{\mathrm{E,D}}(k)$ indicate the electrical impedance signatures under intact (prior to grinding) and damaged (after grinding) condition, respectively; $\overline{Z}_{\mathrm{E,H}}$ and $\overline{Z}_{\mathrm{E,D}}$ are the averaged signatures under the same conditions; and k is the frequency that ranges from ω_I (initial frequency) to ω_F (final frequency).

Baptista et al. [9], by using the EMI technique, tested these same damage indices to investigate the influence of temperature on PZT sensor impedance signatures, which were calculated for the frequency band of 16–40 kHz.

Based on its potentiality and on the results that were obtained by Marchi et al. [11], who conducted a pioneer experimental work with the EMI technique applied on the grinding monitoring of a SAE 1020 steel with a CBN superabrasive grinding wheel, this work aimed to investigate the surface integrity of hardened steel after the grinding operation by using a conventional abrasive wheel and various cutting conditions based on the EMI technique. Microhardness and surface roughness of the machined surfaces, as well as grinding power, were also measured in order to detect any damage in the machined surface and validate the EMI technique.

2 Experimental procedures

Grinding tests were carried out on a semi-precision peripheral surface grinding machine, manufactured by Mello, with 3 hp and 2400 rpm. The workpiece material that was used in this work is the ABNT N2711 steel (40 ± 2 HRc) from Villares Metals [12] with dimensions of 60 mm × 12 mm × 15 mm. It is as good machinability material, which in general possess good response to nitriding and its application comprises structures for plastic, molds manufacturing for injection of non-chlorinated thermoplastics, dies for extrusion, and blowing molds. Its chemical composition is presented in Table 1.

Prior to the grinding tests, a PZT transducer was properly glued on each workpiece surface, whose details are described next. The transducers (PZT sensor/actuator) consisted of a low-cost piezoelectric diaphragm, 7BB-35-3 model from Murata Manufacturing, which were employed in the electromechanical impedance measurement. It consists of a disc-shaped PZT ceramic (active element) with a diameter of 9 mm and thickness of 0.23 mm adhered concentrically on a brass disc with diameter of 12 mm and thickness of 0.30 mm. Before bonding the transducer on the workpiece material surface, two wires were welded on the transducer poles. All the workpiece samples were properly prepared and their ends were machined with sandpaper with mesh in a sequence of 80, 120, and 220 to improve the glue adhesion to the workpiece. Then, the transducer was bonded on the workpiece material surface by using a thin layer of a cyanoacrylate glue as shown in Fig. 1(a). To avoid influence of humidity and coolant during the grinding trials and to improve mechanical resistance of the set, a white silicone rubber from Vonder was used (Fig. 1(b)).

Table 1 Chemical composition (% in weight) of the ABNT N2711 steel grade

C	Mn	Cr	Mo	Ni	V
0.56	0.70	0.70	0.30	1.56	0.075

Six workpiece samples were prepared to the grinding tests and the following input cutting parameters were tested: three cut values of depth (15, 25, and 50 μm) and two workpiece speeds (2.4 and 5 m/min). A cutting speed of 36 m/s was employed, which was kept constant in all the tests. Each test was replicated once. The workpiece material was held in a precision vise from Gin mounted on the grinder table. During the grinding pass, the workpiece motion is first in the opposite direction of the wheel speed (up grinding) and, then, in the same direction (down grinding). The abrasive wheel was a Norton conventional white aluminum oxide (Al_2O_3) with vitrified bond, with designation AA60K6V and with following dimensions: 290 mm × 25.4 mm × 76 mm (outer diameter × width × internal diameter). The setup for the machining tests is shown in Fig. 2.

All the machining tests were carried out with a vegetable-based coolant (Vasco 7000 from Blasser Swisslube). It is a semi-synthetic, water-miscible, recommended for grinding operation, considered a green and environmentally friendly product, which was employed in a proportion of 1:19 (oil to water) and directed to the grinding zone through a traditional nozzle at a flow rate of 8.7 l/min.

A design of experiments (DOE) was employed to select levels of factors through the combination of workpiece speed and radial depth of cut values, that resulted in six input cutting conditions (C1 to C6) as shown in Table 2, according to the following input parameters:

- Workpiece speed (Vw): 2.4 and 5 m/min;
- Radial depth of cut (at each grinding cycle): 10, 25, and 50 μm
- Depth of cut (width of the workpiece surface): 12 mm
- Dressing conditions: a single-point diamond dresser with a point radius of 0.3 mm with a dressing depth of 20 μm and overlap ratio (Ud) of 5.

The output parameters that were investigated in this work were the electromechanical impedance (EMI) measurements, microhardness, and surface roughness of the machined surfaces. Also, all the samples were visually examined, with the aid of an optical microscope Olympus Evolution LC Color SZ6145TR model having a digital camera that is attached to a computer and image analysis software (Image-Pro Express 5.1) with magnification of × 45 to detect occurrence of burning or other superficial thermal damages.

2.1 Measurement of the electromechanical impedance

The EMI measurements were performed by using the system described by Baptista and Filho [13]. In the present work, the method was applied to determine the frequency ranges in

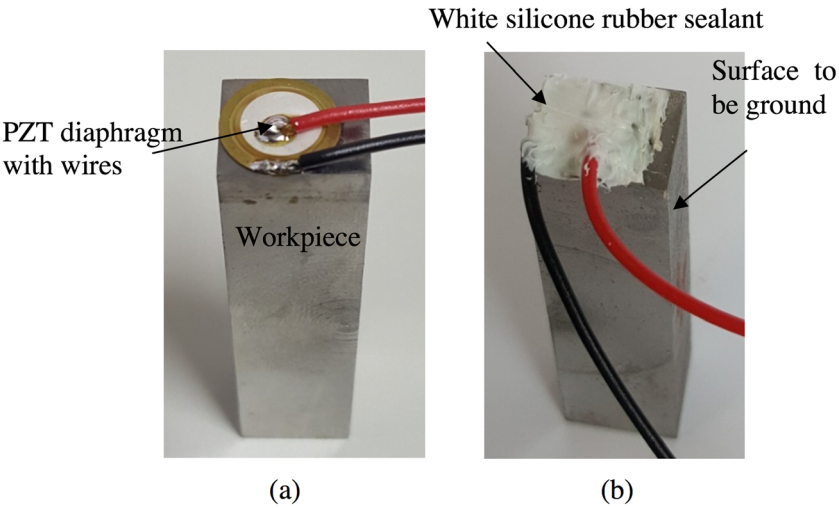

Fig. 1 Stages of the preparation and bonding of the PZT diaphragm on the workpiece material (N7711 steel grade): (a, b) PZT coated with a white silicone rubber

which the PZT transducers are more sensitive for damage detection from the grinding operation. For this purpose, the signals were measured prior and after the grinding operation in a laboratory having an appropriated bench tests (personal computer, USB DAQ device, thermocouple, wall-mounted air conditioner device, polystyrene box, thermometer, and LabVIEW software); that is. the workpieces materials were removed from the grinder machine for EMI measurements to eliminate external influences and correlating signals only to the mechanical proprieties of the workpieces.

2.1.1 Electric system for EMI data acquisition

Regarding the test bench to collect EMI signatures, as described by Baptista and Vieira [14] and Marchi et al. [11], the system is based on a multifunction USB DAQ device with one digital-to-analog converter (DAC), which is responsible to generate the excitation signal $x(t)$, and an analog-to-digital (ADC) converter, which acquires the response signal $y(t)$ from the PZT transducer. The EMI system, which is shown in Fig. 3, also contains a R_S precision resistor that is connected to the transducer and aims to limit the current. Both control and operation of EMI measurements were developed in a specific routine programming developed in a LabVIEW platform in accordance with the one proposed by Baptista and Filho [13]. Finally, the electrical impedance signatures $Z_E(\omega)$ can be obtained from the frequency response function (FRF), $H(\omega)$ (this is calculated from the discrete Fourier transform (DFT) of the digitized $x[n]$ and $y[n]$ signals corresponding to the analog excitation and response signals of the transducer, respectively). A fast Fourier transform (FFT) algorithm is used to calculate the DFT function.

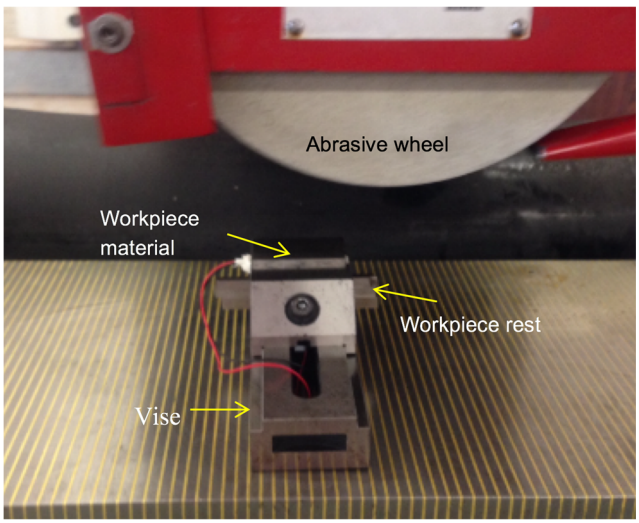

Fig. 2 Experimental setup of grinding the N2711 steel workpiece with a mounted PZT transducer

2.1.2 Experimental setup for EMI measurement

Experimental data acquisition for EMI technique was performed with the aid of a USB-6221 DAQ device from National Instruments, which was connected to a USB port of the personal computer (Intel Core 2 3600, 4 GB), running the Windows operational system and containing the LabVIEW

Table 2 Experimental design for the grinding tests

Cutting parameters, condition (C)	Cutting speed, Vs [m/s]	Workpiece speed, Vw [m/min]	Radial depth of cut, a_e [μm]	Wheel width (in contact with workpiece surface), b_s [mm]
C1	36	2.4	15	12
C2			25	
C3			50	
C4		5	15	
C5			25	
C6			50	

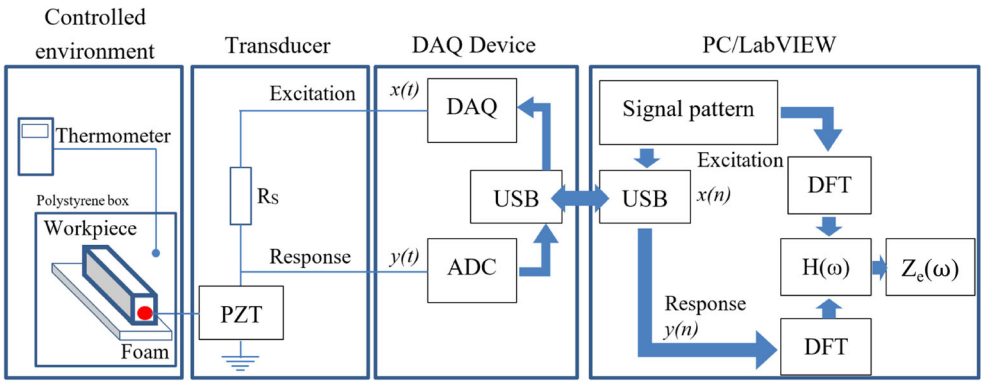

Fig. 3 Schematic illustration for the electromechanical impedance data acquisition system employed in monitoring of workpiece damage (adapted from [14])

package. A sampling rate of 256 kS/s (kilo-samples/second) was selected, which resulted in a Nyquist frequency of 125 kHz. This sampling rate is 75% lower than that employed by Marchi et al. [11] in their experimental work of grinding monitoring. However, such frequency does not adversely affect the results, because the maximum frequency previously observed was of about 100 kHz, ensuring the Nyquist criterion. The setup for electromechanical impedance measurement is shown in Fig. 4. The DAQ system generates a chirp signal with magnitude of 1 V, which ranges from 0 to 125 kHz. In this way, the transducer is excited for a wide spectrum, which generates waves throughout the workpiece and the response is simultaneously collected by the transducer.

After the complete assembly and adjustments of the acquisition system, a wall-mounted air conditioner device was switched on until the laboratory reaches a temperature below 24 °C. So, the workpiece material to be tested was placed on a piece of foam to avoid vibrations and inside a polystyrene box to keep the temperature constant (Fig. 4). In the sequence, the polystyrene box was closed and then the air conditioner device was switched off. When the temperature reached 24.0 °C, then the EMI measurement was started. The temperature was monitored using a thermometer, MT-455 model from Minipa (with a resolution of 0.1 °C and a basic accuracy of 0.1%), and a type K thermocouple. Three impedance measurements were collected for each workpiece material, alternating among the N2711 steel workpieces. For each measurement, the software automatically performs five internal measurements and calculates an average value. Consequently, for each workpiece condition, an average signature from 15 impedance measurements was calculated. An average signature was obtained prior to the grinding operation and other signatures after the grinding operation. The RMSD and CCDM damage indices were calculated for the signatures after the grinding in relation to the signatures prior the grinding (baseline). For such calculations, several bands were tested considering ranges of 5 to 10 kHz for the real part of the impedance. Finally, the indices for all the frequency ranges were compared to microhardness, roughness, and grinding power measurements to find a correlation.

2.2 Visual inspection and measurements of surface roughness of the machined surfaces

After grinding, all the samples were properly cleaned with hydrated alcohol and air-dried for measurements of the surface roughness and microhardness. Initially, all the machined surfaces were visually inspected and then taken to be examined in an optical microscope, from Olympus, SZ6145TR model, with an attached digital camera.

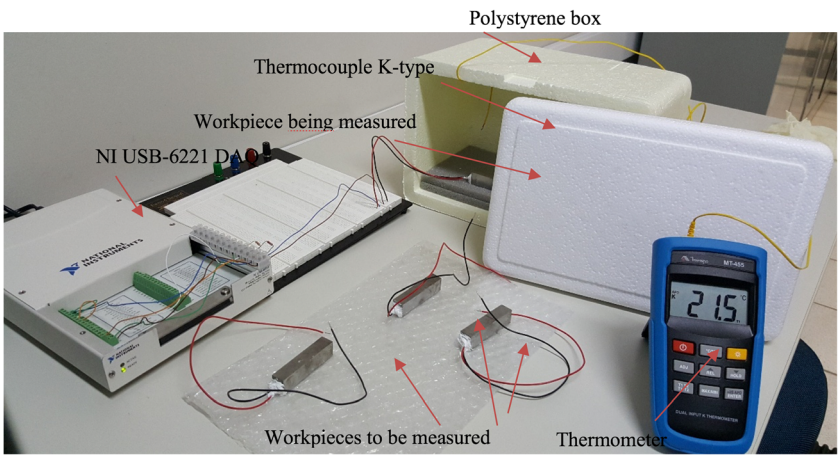

Fig. 4 Setup for the EMI measurements of N2711 steel workpieces

The surface roughness (Ra parameter—arithmetic mean roughness value) was recorded after each grinding cycle with the aid of a Mitutoyo SJ201P portable stylus-type instrument by positioning it perpendicular to the feed marks on the ground surface (Fig. 5). The measurements were carried out in laboratory where the average room temperature was 20 (± 1.0) °C. Cutoff and evaluation lengths of 0.8 and 5 mm, respectively, were selected. Three equidistant measurements were taken along the length of the machined surface and the average of measurements was calculated. This average represents the surface roughness value of the machined surface for each cutting condition. Ra parameter was selected in this work because it is universally employed as an international roughness evaluation parameter for machined surfaces.

2.3 Microhardness measurements

The microhardness measurements were taken with the aid of a Mitutoyo microhardness tester, HM-200 model with a load of 1.981 N (HV0.2) for 10 s. They were taken on the machined surface in nine different points as shown in the schematic illustration in Fig. 6. The first measurement was taken in the region in which the abrasive wheel enters on the workpiece material and at 10 mm distant from the starting edge. From Fig. 6, the region highlighted was taken as reference to the analysis. A surface with the coordinates of the measurements in x and y axes and the respective microhardness value in the z axis were generated with the aid of the MATLAB software from MathWorks. By applying a color scale with values interpolated along the surface, microhardness graphs were then obtained as shown in the next section.

2.4 Grinding power measurement

The grinding power values were recorded through electric current and voltage signals. HAS 50–600-S and LV 20-p sensors were employed for the measurements of electric current and voltage signals and then the results were processed through NI LabVIEW software. The results represent the average of values recorded during a grinding pass of the abrasive wheel on the workpiece material surface.

Fig. 5 Measurement of the surface roughness of steel workpiece

3 Results and discussion

Results and discussion for the output variables (EMI signatures, microhardness, surface roughness, and grinding power) after grinding the N2711 steel grade under various cutting conditions are presented in this section.

3.1 Images of the machined surfaces and microhardness plots

The machined surface and the microhardness graphs are disposed in Fig. 7, columns 1 and 2, respectively. The microhardness of the workpieces was also measured prior to grinding operation, so they are considered in this work as reference value and equal to 500 ± 10 HV.

From Fig. 7, column 1, it is possible to observe the images of ground workpieces under the machining conditions C2, C3, and C6 (based on Table 2), which correspond to the lowest workpiece speed (2.4 m/min), C2 and C3, as well as to that with the highest depth of cut (C3 and C6), i.e., most severe machining conditions. From Fig. 7, column 2, it is noted that the highest microhardness values were recorded in the regions covered with an oxide layer, again C2, C3, and C6 conditions. After the grinding operation, microhardness values are above or below the reference measured value, thereby evidencing that changes occurred in the microstructure of the workpiece material as consequence of the intense flux of heat generated during grinding; as in this case, it was transferred to the workpiece surface. According to Malkin and Guo (2008), the high temperatures that are reached during the process can cause various types of thermal damage to the workpiece, such as burning, phase transformation, and softening (tempering) of the surface layer with possible rehardening. By comparing the ground workpiece with microhardness plots, it is evident that surfaces experienced a rehardening because of the high microhardness values recorded after grinding when compared to reference value. Although the machined surfaces exhibited regions with oxide formation, the microhardness values of the ground workpiece material with the conditions C1, C4, and C5 were close to the reference value.

3.2 Surface roughness values

Figure 8 shows the results of surface roughness (Ra parameter) as a function of radial depth of cut (a_e) and different workpiece speed values. It can be seen that surface roughness increased with the radial depth of cut, as expected, regardless of the workpiece speed. When radial depth of cut is increased,

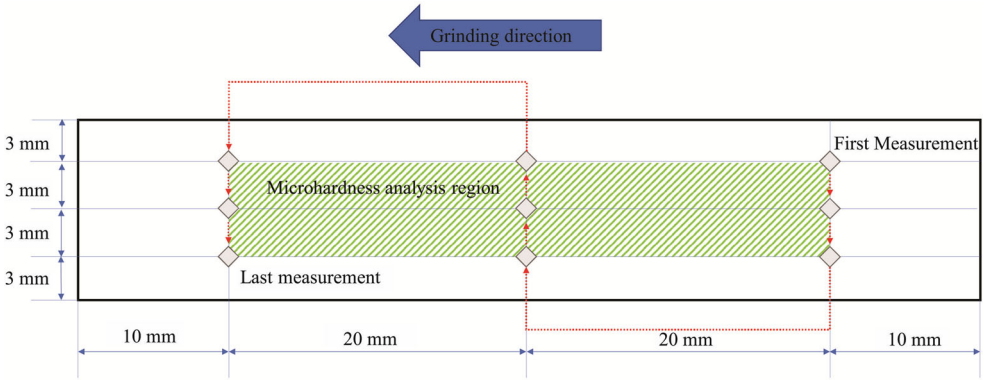

Fig. 6 Trajectory of the microhardness measurement and of the analysis region on the N2711 steel surface after grinding

the contact area between workpiece material and grits from the abrasive wheel also increases. This increases the workpiece material area under deformation and leads to higher heat generation in the grinding zone. As a consequence, the workpiece

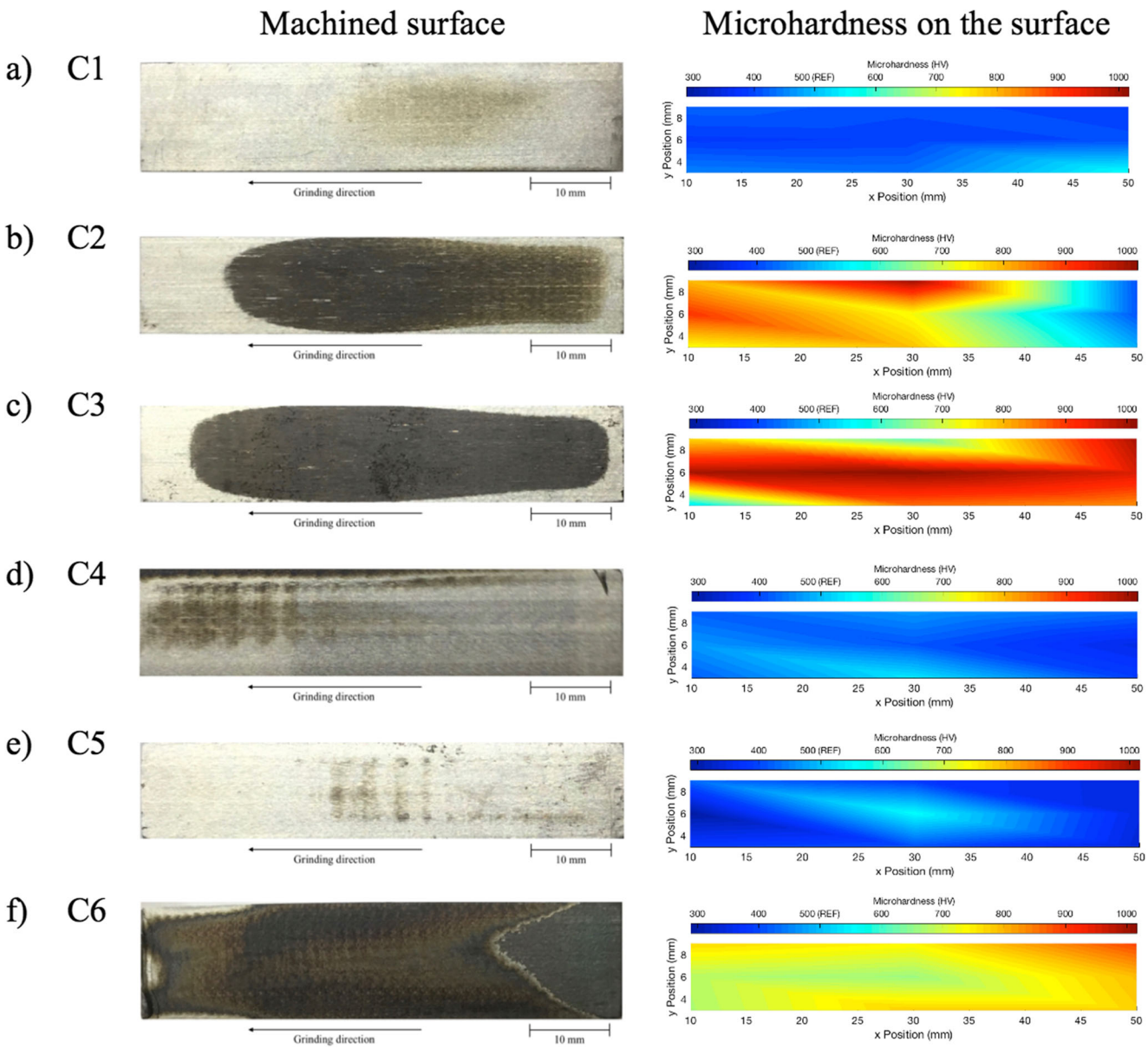

Fig. 7 Images of the surfaces and plots of the microhardness on the surface of ABNT N2711 steel after grinding in various cutting conditions

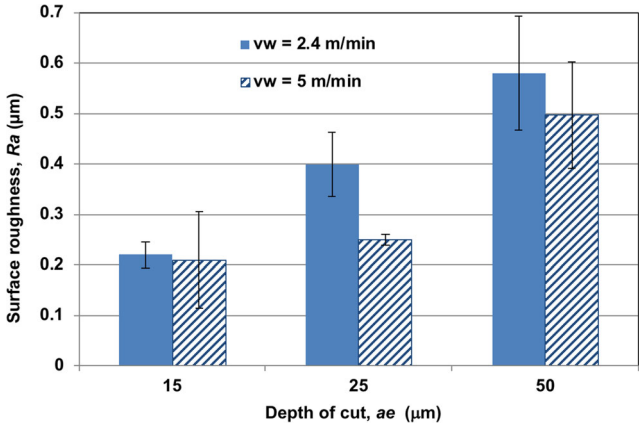

Fig. 8 Surface roughness after grinding N2711 steel with different cutting conditions

surface experiences thermal expansion and outward surface movements towards the wheel in the point where higher temperatures are being developed, thereby resulting in high quality on surface finish of the component [15, 16]. The more severe is the cutting condition, the higher is the plastic deformation during grinding, which increases the number of irregularities on the workpiece surface, thus contributing to deterioration of the surface roughness. De Paiva et al. [17] conducted an investigation about the influence of coolant concentration and flow rate on surface roughness of two materials for production of plastic injection molds with close hardness of the workpiece material and with similar cutting conditions as those tested in this current investigation. In their work, they reported that Ra parameter was more sensitive to the variation of radial depth of cut (a_e) than with the coolant concentration. The authors also reported that Ra parameter increased with depth of cut. It is important to highlight that surface roughness affects workpiece fatigue strength when it is subjected to loads as well as is determining in assembling of parts where it required precision fits, among others [18]. Also, all the Ra values are lower than 0.6 μm, below the stipulated rejection limit of 0.63 μm for the grinding process generally reported in the literature. Such results indicate that cutting parameters were appropriated for grinding of an ABNT N2711 steel with a conventional abrasive wheel.

Surface roughness is also dependent on the workpiece speed in grinding, as shown in Fig. 8. It can be observed that surface roughness decreases as workpiece speed (Vw) increases and this was more evident after grinding with the depth of cut of 25 μm, where Ra was about 38% lower in average after employing Vw = 5 m/min. Such phenomenon can be associated to the shortest contact time between the workpiece material and grinding wheel when grinding at the highest workpiece speed value. According to Lavine and Jen [19], a workpiece material is less susceptible to less thermal damage during grinding, and consequently poor finish, if workpiece speed is increased.

3.3 Grinding power

According to Malkin and Guo [3], prediction and control of workpiece thermal damage can be feasible through grinding power monitoring. From Fig. 9, it can be seen that, similar to the behavior observed for surface roughness (Fig. 8), grinding power increased with depth of cut values, irrespective of workpiece speed. As previously mentioned, the grinding contact area between the workpiece material and abrasive wheel increases with depth of cut (specific grain cutting depth) and causes the both normal and tangential components cutting forces to be increased, thereby requiring more power to form chip [20]. Also, Aguiar et al. [21] reported during their investigation of the threshold to identify workpiece burning in peripheral grinding of a SAE 045 steel conventional aluminum oxide abrasive wheel that once the surface burning occurs, a metallic particle adhesion growth in the abrasive grains of the grinding wheel will be intensified, thereby increasing cutting forces and consequently the grinding power, as well as adversely affecting the surface finish of the machined component. In case of hardened steels, such as SAE 52100 steel grade that is employed in bearing components manufacturing, Malkin and Guo [3] reported that surface burning generated in grinding operation can reduce the workpiece material limit of fatigue strength and consequently its service life. By comparing the microhardness of machined surfaces with the grinding power results, it can be noted that those workpiece surfaces that experienced hardness increasing also demanded high grinding forces.

With regard to the influence of the workpiece speed in the grinding power, from the standard deviation values, it can be inferred that there is no difference between the low and high values employed for all the depth of cut values tested.

3.4 Electromechanical impedance

The impedance signatures were obtained through the EMI technique for every workpiece before and after the grinding.

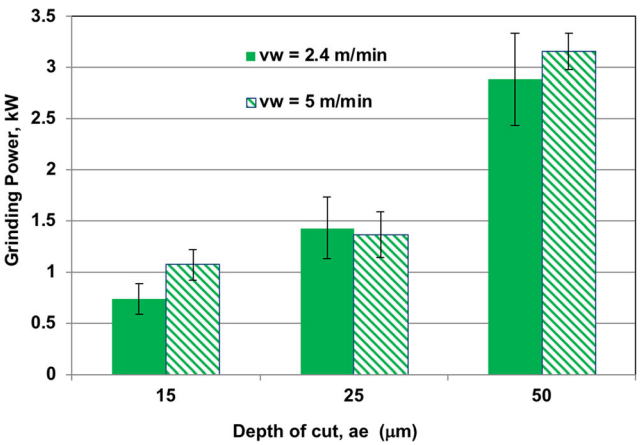

Fig. 9 Grinding power recorded during grinding N2711 steel under various cutting conditions

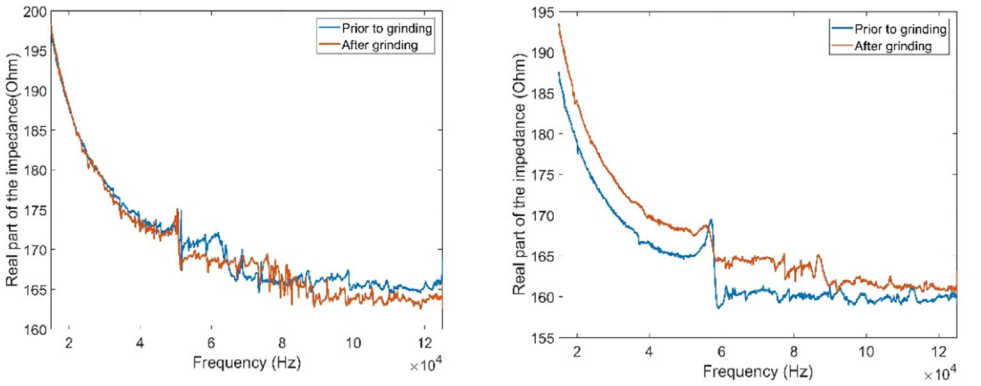

a) C1 condition: *ae* = 25 μm and *vw* = 5 m/min

b) C5 condition: *ae* = 50 μm and *vw* = 5 m/min

Fig. 10 Impedance signatures provided by the PZT on the N2711 steel before and after the grinding operation

Figure 10 shows the real part of the impedance signatures for two conditions, C1 and C5, as an example. The blue curve represents the signature measured prior to grinding and the red after the grinding. By observing such graphs, it is noted that C5 presented a higher difference between the two curves. That was expected because, despite C1 and C5 having the same workpiece speed, C5 has the biggest cut of depth. It is important to note that the frequencies which were considered to analyses was from 15 to 125 kHz and the higher the frequency, the lower the impedance, which represents a capacitive behavior of the system.

The damage indices RMSD and CCDM were calculated considering both curves, red and blue, for every condition, in different frequency ranges. By observing the results previously described for the images, microhardness, surface roughness, and grinding power, the best damage index in a specific frequency band was chosen, according to the best correlation that was observed. The CCDM index for the frequency 65–75 kHz, shown in Fig. 11, presented the best correlation with the other parameters, and the higher the depth of cut, the higher the value of the index. By observing only the blue bars, i.e., keeping the workpiece speed constant, the index increases when the depth of cut increases, which represent an increase also of the damage. This happens because the CCDM index is related to the difference in the shape between the both signatures, and the higher the difference between the curves, the higher the index. The same behavior can be observed for the yellow bars.

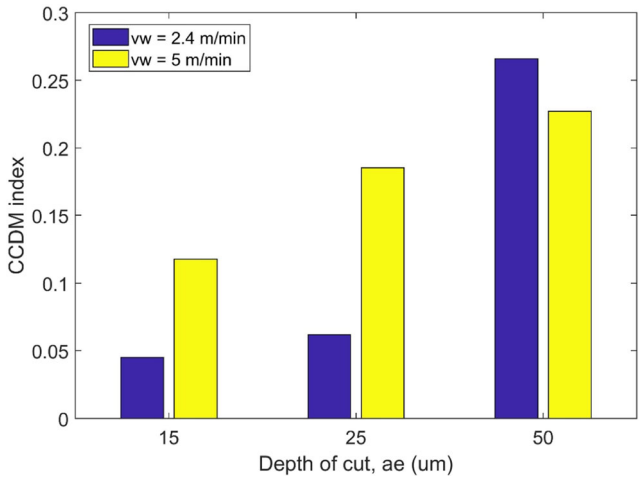

Fig. 11 CCDM index for the frequency band of 65–75 kHz under various cutting conditions

4 Conclusions

The following conclusions can be drawn from this investigation:

- The correlation coefficient deviation metric (CCDM) damage index for the frequency band of 65–75 kHz presented the best correlation with the mechanical parameters, which increased with depth of cut value, following the same trend of the surface roughness and grinding power parameters;
- CCDM index proved to be sensitive to identify the depth of cut variation, when the workpiece speed is kept constant. Also, this index increased with the depth of cut;
- With regard to the microhardness on the ground workpieces, they were affected by the machining conditions and the highest values were recorded in the regions with an oxide layer on the surface. That result is coincident with the grinding conditions in which combination of depth of cut (ae) in excess of 15 μm and the lowest workpiece speed, Vw = 2.4 m/min.
- Surface roughness values (Ra parameter) increased with depth of cut, irrespective of the tested workpiece speed. They were kept below the stipulated rejection limit of 0.63 μm for grinding operations commonly reported in the literature;

- Grinding power increased with depth of cut values, irrespective of workpiece speed, following the same behavior observed for surface roughness parameter. Grinding power showed to be less sensitive to the variation on the workpiece speed under the conditions investigated;
- From overall results, the EMI technique tested in this work was able to detect alterations on the ground surfaces of the ABNT N2711 steel under the conditions investigated. A close correlation among EMI technique and the surface roughness and the grinding power was identified, thereby demonstrating that such technique was viable in monitoring workpiece surface damages in grinding.

Acknowledgements The authors thanks initially the Department of Electrical Engineering of Faculty of Engineering Bauru (Universidade Estadual Paulista (UNESP), Sao Paulo, Brazil) and School of Mechanical Engineering of Federal University of Uberlandia, MG, Brazil, for enabling the development of the research that resulted in this work. One of authors, Rosemar Batista da Silva, thanks the Post-Graduate Program of Electrical Engineering of FEB-UNESP-BAURU for the all the laboratory facilities and support, as well as CAPES for the concession of the PNDP post-doctoral scholarship at the Post-Graduate Program of Electrical Engineering of FEB-UNESP-BAURU (2016–2017). The same author also is grateful to the Federal University of Uberlandia (Brazil) for approving his post-doctoral leave.

Compliance with ethical standards

Conflict interest The authors declare that there is no conflict of interest.

References

1. Rowe WB (2010) Modern grinding techniques. Mod Grind Tech. https://doi.org/10.1002/9780470882313
2. Irani RA, Bauer RJ, Warkentin A (2005) A review of cutting fluid application in the grinding process. Int J Mach Tools Manuf 45: 1696–1705. https://doi.org/10.1016/j.ijmachtools.2005.03.006
3. Malkin S, Guo C (2008) Grinding technology—theory and applications of machining with abrasives, second. Industrial Press, New York
4. Field M, Kahles JF, Cammett JT (1972) A review of measuring methods for surface integrity. CIRP Ann - Manuf Technol 21: 219–238
5. Ullah AMMS, Caggiano A, Kubo A, Chowdhury MAK (2018) Elucidating grinding mechanism by theoretical and experimental investigations. Materials (Basel) 11. https://doi.org/10.3390/ma11020274
6. Caggiano A, Teti R (2013) CBN grinding performance improvement in aircraft engine components manufacture. Procedia CIRP 9: 109–114. https://doi.org/10.1016/j.procir.2013.06.177
7. Klopfstein MJ, Lucca DA (2011) Recent assessment of surface integrity resulting from fine finishing processes. Procedia Eng 19: 209–221. https://doi.org/10.1016/j.proeng.2011.11.103
8. Annamdas VG, Radhika MA (2013) Electromechanical impedance of piezoelectric transducers for monitoring metallic and non-metallic structures: a review of wired, wireless and energy-harvesting methods. J Intell Mater Syst Struct 24:1021–1042. https://doi.org/10.1177/1045389X13481254
9. Baptista F, Budoya D, Almeida V, Ulson J (2014) An experimental study on the effect of temperature on piezoelectric sensors for impedance-based structural health monitoring. Sensors 14:1208–1227. https://doi.org/10.3390/s140101208
10. Bhalla S, Soh C-K (2012) Electro-mechanical impedance technique. In: Smart materials in structural health monitoring, control and biomechanics. In: Adv. Top. Sci. Technol. China. Springer, Berlin, Heidelberg, p 17–51
11. Marchi M, Baptista FG, de Aguiar PR, Bianchi EC (2015) Grinding process monitoring based on electromechanical impedance measurements. Meas Sci Technol 26:045601. https://doi.org/10.1088/0957-0233/26/4/045601
12. Villares Metals (2017) Plastic mold steel - N2711M grade
13. Baptista FG, Filho JV (2010) Optimal frequency range selection for PZT transducers in impedance-based SHM systems. IEEE Sensors J 10:1297–1303. https://doi.org/10.1109/JSEN.2010.2044037
14. Baptista FG, Vieira JF (2009) A new impedance measurement system for PZT based structural health monitoring. IEEE Trans Instrum Meas 58:3602–3608
15. Marinescu I, Hitchiner M, Uhlmann E (2006) Handbook of machining with grinding wheels. Vasa. https://doi.org/10.1007/s13398-014-0173-7.2
16. Marinescu JD, Rowe WB, Dimitrov B, Inasaki I (2004) Abrasives and abrasive tools. Tribol Abras Mach Process:369–455. https://doi.org/10.1016/B978-1-4377-3467-6.00009-4
17. de Paiva RL, da Silva RB, Jackson MJ, Abrão AM (2017) The influence of cutting fluid concentration on surface integrity of VP80 steel and the influence of cutting fluid flow rate on surface roughness of VPATLAS steel after grinding. J Manuf Sci Eng 139: 121003. https://doi.org/10.1115/1.4038149
18. Wang X, Feng CX (2002) Development of empirical models for surface roughness prediction in finish turning. Int J Adv Manuf Technol 20:348–356. https://doi.org/10.1007/s001700200162
19. Lavine AS, Jen TC (1991) Coupled heat transfer to workpiece, wheel, and fluid in grinding, and the occurrence of workpiece burn. Int J Heat Mass Transf 34:983–992. https://doi.org/10.1016/0017-9310(91)90009-4
20. Sutowski P (2017) The effect of process parameters on grinding forces and acoustic emission in machining tool. J Mech Energy Eng 1(41):37–44
21. Aguiar PR, de Dotto FRL, Bianchi EC (2005) Study of thresholds to burning in surface grinding process. J Brazilian Soc Mech Sci Eng 27. https://doi.org/10.1590/S1678-58782005000200007